Journal of The Electrochemical Society, 2024 **171** 055502

Bacterial-Polyhydroxybutyrate for Biocompatible Microbial Electrodes

Lilian Danielle de Moura Torquato,[1,2,3] Dario Lacalamita,[1] Rosa Maria Matteucci,[4] Jefferson Honorio Franco,[1] Rossella Labarile,[5] Alberto Perrotta,[6] Massimo Trotta,[5] Gianluca Maria Farinola,[1] Maria Valnice Boldrin Zanoni,[2,3] Matteo Grattieri,[1,5,*,z] and Paolo Stufano[6,z]

[1]*Department of Chemistry, Università degli Studi di Bari "Aldo Moro," Bari 70125, Italy*
[2]*Institute of Chemistry, São Paulo State University (UNESP), Rua Prof. Francisco Degni, São Paulo 14800-060, Brazil*
[3]*National Institute for Alternative Technologies of Detection, Toxicological Evaluation and Removal of Micropollutants and Radioactives (INCT-DATREM), São Paulo State University (UNESP), Rua Prof. Francisco Degni, São Paulo 14800-060, Brazil*
[4]*Dipartimento di Ingegneria Elettrica e dell'Informazione, Politecnico di Bari, Bari 70125, Italy*
[5]*Istituto per i Processi Chimico Fisici (CNR-IPCF), Consiglio Nazionale delle Ricerche, Bari, 70125, Italy*
[6]*Institute of Nanotechnology, (CNR-NANOTEC), Consiglio Nazionale delle Ricerche, Bari, 70125, Italy*

The development of bioelectrochemical systems requires careful selection of both their biotic and abiotic components to obtain sustainable devices. Herein, we report a biophotoelectrode obtained with polyhydroxybutyrate (PHB), a biopolymer, which purple non-sulphur bacteria produce as an energy stock under specific environmental conditions. The electrode was obtained by casting a mixture composed of PHB and carbon fibers in a 3:2 mass ratio. Following, the composite material was modified with polydopamine and thermally treated to obtain a hydrophilic electrode with improved electrochemical behavior. The bio-based electrode was tested with metabolically active cells of *Rhodobacter capsulatus* embedded in a biohybrid matrix of polydopamine. The system achieved enhanced catalytic activity under illumination, with an 18-fold increase in photocurrent production compared to biophotoelectrodes based on glassy carbon, reaching a current density of 12 ± 3 μA cm^{-2}, after 30 min of light exposure at +0.32 V. The presented biocompatible electrode provides a sustainable alternative to metal-based and critical raw material-based electrodes for bioelectrochemical systems.
 [DOI: 10.1149/1945-7111/ad40d6]

Manuscript submitted January 26, 2024; revised manuscript received April 11, 2024. Published May 3, 2024. *This paper is part of the JES Focus Issue on Trends and Biohybrid Approaches in Microbial Electrochemical Systems.*

Microbial electrochemical systems (MES) are biohybrid devices where the catalytic activity of microorganisms is combined with electrodes for obtaining fuel cells, biosensors, and the synthesis of valuable chemicals.[1–4] In recent years, particular interest has been posed in the application of photosynthetic organisms in MES to enable the conversion of light energy into electrical and chemical energy.[5–14] However, electrode materials utilized in these biohybrid devices are rarely biobased, while utilizing a material of biological origin opens a new way to further increase the sustainability of the MES. Specifically, electrode materials are often selected focusing on their intrinsic catalytic properties, such as Pt,[15] Pd,[16] Ru/Fe,[17,18] Ni,[19–21] Ti[22–24] based electrodes but carbon-based materials are highly desirable as well as more biocompatible and sustainable approaches.[25–35] Particular attention has been posed to providing an efficient electrode combining desired surface and structural properties, thus designing new conductive and biodegradable materials for high biocompatibility and electrochemical performance. In this context, the use of biobased polymers coupled with conductive material was reported by Atanassov et al., showing an efficient bacterial colonization with pure cultures of *Shewanella oneidensis*, and an enhanced catalytic activity.[36,37] Recently, urethane has been proposed as an electrode in microbial fuel cells (MFCs) due to its large surface area, flexibility, and stability over time.[38] Nevertheless, this material is nonconducting, requiring the development of urethane containing activated carbon powder and carbon nanotubes. The MFCs generated a maximum power density of 28.27 μW cm^{-2} using a microbial community present in soil and cow manure. The result obtained shows that the use of plastic polymer and conductive material together is a promising approach for bioelectrochemical purposes.

Polyhydroxyalkanoates (PHAs), polylactic acid (PLA), and polybutylene succinate (PBS) are an important class of bio-based polymers that have the potential to progressively replace traditional plastics due to their comparable physical, chemical, thermal, and mechanical properties.[39] However, in comparison to PLA and PBS, which are produced upon polymerization of their monomers, PHA polymerization is performed by bacteria. Specifically, purple non sulphur bacteria, such as *Rhodobacter capsulatus* (*R. capsulatus*), *Rhodobacter sphaeroides* and *Rhodobacter palustris*, accumulate poly-3-hydroxybutyrate (PHB) as reserve polymer in nutrient limited conditions.[40–44] PHB is a short chain length PHA with characteristics akin to petroleum based polymers, such as insolubility in water, good resistance to UV rays, stiffness, high degree of polymerization, and thermoplasticity.[45] Due to its physico-chemical properties and biodegradability, PHB is mostly used for the production of disposable items, food packaging materials,[39] and medical applications.[46] However, PHAs are not conductive polymers, leading to their coupling with gold nanoparticles[47] and carbon nanotubes[48] to develop composite material for electrochemical purposes. In this regard, the coupling of PHA with carbon nanofibers (CF) has interesting features, due to the large surface area of CF, their reasonable conductivity, and chemical/thermal stability.[49,50]

The design of a polyhydroxybutyrate-carbon nanofiber (PHB-CF) based bioelectrode is a step forward in the development of MES that requires a combination of highly biocompatible materials with an efficient connection with biocatalysts. The prototypal PHB-based electrode prepared using an ink-PHB-CF mixture on paper support[51] utilized with photosynthetic bacteria showed increased current densities compared to the glassy carbon-based hybrid electrode. However, it also suffered from unstable performance and high background electrochemical noise. The bacterium utilized to obtain biophotoelectrodes was the photosynthetic purple non sulphur bacterium *R. capsulatus*, a model organism, due to its versatile metabolism that allows application in bioremediation,[52,53] H_2

*Electrochemical Society Member.
[z]E-mail: matteo.grattieri@uniba.it; paolo.stufano@cnr.it

production,[54,55] and biosensing.[53,56] *R. capsulatus* photoelectrocatalysis has been consistently studied in the last decade with various artificial approaches facilitating the photo-induced electron transfer,[51,57–61] and also in the presence of environmental stresses, such as high salinity[62] and xenobiotic compounds (i.e., benzoic acid, nitrophenols, and halogenated aromatics).[63] Herein, we report a free-standing biobased electrode composed of PHB and CF with high conductive properties and biocompatibility thanks to a surface thermal treatment with polydopamine. The electrode is utilized with *R. capsulatus* to obtain a biophotoelectrode with improved stability and photocurrent generation, paving the way for the development of biohybrid devices following a circular economy and waste reduction approach.

Experimental

Chemicals.—Dopamine hydrochloride (MW = 189.64 uma, CAS 62–31–7) and conical carbon nanofibers were purchased from Sigma Aldrich. Polyhydroxybutyrate (ENMAT™ Thermoplastics Resin Y3000P) was supplied by Tianan Biopolymer in the form of pellets which were used as received. All other chemicals used in this study were used as received without further purification. All solutions were prepared using ultrapure Milli-Q water (18 MΩ cm^{-1}).

Polyhydroxybutyrate - Carbon nanofibers (PHB-CF) electrode.—The procedure for the electrode preparation via the casting process is reported in Scheme 1. Specifically, 360 mg of polyhydroxybutyrate (PHB) and 240 mg of carbon nanofibers (CF) (3:2 mass ratio) were mixed in 20 mL of dichloromethane (CH_2Cl_2). The obtained suspension was heated at 100 °C and stirred at 700 rpm (Velp Scientifica Are heating magnetic stirrer) for 1 h and subsequently cast in a Petri dish. After evaporation of the solvent, the obtained composite flat material was cut into slices of the desired dimension for use in the electrochemical cell as a substrate electrode (1.5 cm × 0.5 cm × 1 mm). The electrodes were washed thoroughly with ethanol to remove any impurities before dip in a polydopamine suspension, obtained by aerobic polymerization of a 5 mM dopamine solution for 1 h in MOPS buffer (pH 8), completely covering the surface of the material. The electrodes finally underwent a thermal treatment at 170 °C for 1 h and were stored at room temperature until use.

Electrode characterization.—The electrode surface wettability was characterized by measuring the static Water Contact Angle (WCA) using a CAM 200 digital goniometer (KSV instrument). For each measure, a 2 μL drop of Milli-Q water was deposited, and the relevant image was acquired. WCA values were calculated using KSV CAM 2008 software for image analysis.

Bacteria growth.—*Rhodobacter capsulatus* strain DSMZ 152 was obtained from Deutsche Sammlung von Mikroorganismen and Zellkulturen GmbH (DMSZ). Bacterial cells were grown for 72 h under photoheterotrophic semi-anaerobic conditions using malic acid as a carbon source. The growth procedure was performed at 28.0 ± 0.4 °C, using an incubator (IKA KS 3000 i control) without shaking. The illumination was provided by a halogen lamp (80 W).[51,63]

PHB-CF-R. capsulatus photoanode preparation.—The bacterial cells were prepared as previously reported by our group.[51] Shortly, after 72 h of growth, *R. capsulatus* cells were collected and underwent different centrifugation steps. Finally, 50 μL of a 1:1 volume ratio bacteria:polydopamine suspension (1 g mL^{-1} bacterial cells:5 mM dopamine) was spotted onto the PHB-CF electrode, covering a geometric surface area of 0.5 cm^2 and allowed to dry for 1 h. The bioelectrode was finalized by electrochemical polymerization performed with repeated cyclic voltammetry at a scan rate of 20 mV s^{-1} in a potential window of −0.13 V to 0.52 V vs Ag|AgCl (3 M NaCl).

Control electrodes with heat-treated cells or in the absence of bacterial cells were prepared to confirm both the biotic origin of the photocurrent and the role of the PDA matrix for photoinduced electron transfer. The electrode with metabolically inactive cells was obtained by heat-treating *R. capsulatus* cells at 120 °C for 3 h and using the obtained suspension to prepare the bioelectrode as described for the active cells. Accordingly, the bare PDA-modified electrode was obtained spotting 50 μL of the PDA suspension after the aerobic polymerization onto the electrode surface of 0.5 cm^2.

Morphological characterization.—The cell samples embedded in PDA deposited onto the PHB-CF electrodes were fixed adding a solution of 2.5% glutaraldehyde in phosphate buffer for 2 h at room temperature. Afterward, the cells were washed with phosphate buffer three times for 15 min each wash. The washing process was followed by serial dehydration using ethanol at 25%, 50%, 75%, 95%, and 100% for 5 min each. After the dehydration process, the PHB-CF-*R. capsulatus* photoanode was air dried overnight. Samples were mounted on the stainless-steel sample holder and gold sputtered before analysis. Scanning Electron Microscopy (SEM) analysis was performed with a Zeiss-Sigma Field Emission-Scanning electron microscope (Carl Zeiss Co., Oberkochen, Germany) operating at 5 kV and equipped with an in-lens secondary electron detector.

Electrochemical setup.—A three-electrode electrochemical cell was utilized, with the PHB-CF-*R. capsulatus* bioanode as the working electrode (or the different control electrode previously described), a Pt foil as the counter electrode, and an Ag|AgCl (3 M NaCl, Basi MF 2502) as the reference electrode. All potentials in this work refer to this reference electrode in 30 mL of 50 mM malic acid, 10 mM magnesium chloride ($MgCl_2$), and 20 mM MOPS. At least three independent replicate experiments were performed for all the different setups. Photobioelectrocatalysis for *R. capsulatus* was investigated using cyclic voltammetry and chronoamperometry experiments (PalmSens4). Prior to conducting the studies, the electrolyte was purged with Argon (Rivoira UN1006 compressed Argon 99% pure) for 20 min to obtain anaerobic conditions in the electrochemical cell. Illumination was provided using a fiber optic lamp (Schott KL 1500 lCD) equipped with a 10 W bulb, generating an output light intensity of 153 mW cm^{-2} (measured with Gigahertz-Optik MSC15). Chronoamperometry experiments were performed at the potential of +0.32 V to ensure a sufficient overpotential for the oxidation of the polydopamine matrix, alternating light/dark conditions every 200 s. For further evaluation of the developed electrode material, this was compared with commercial glassy carbon performing chronoamperometry experiments, prepared as previously described (maintaining the same volume/surface ratio) All the electrochemical experiments were performed in triplicate both for the biophotoanode and control electrodes (Figs. S2–S5). The biophotocurrent generation was evaluated by subtracting the current obtained under the dark condition from the current under illumination at the fourth illumination cycle when the quasi-steady current generation was achieved. Additionally, for an evaluation of the bioelectrode stability over time, a comparison of the performance between the fourth and eighth illumination cycles were also conducted. All the results are presented following the IUPAC convention.

Attenuated total reflectance–fourier transform infrared (ATR-FTIR) spectroscopy.—To confirm the presence of polydopamine on the electrode surface, ATR-FTIR spectra were recorded with a Perkin Elmer spectrometer (FTIR Spectrum Two, Waltham, MA, USA) at the resolution of 4 cm^{-1}. A total of 16 scans were performed on four different samples (PHB-CF bare electrode, PHB-CF heat treated electrode, PHB-CF with PDA before and after electropolymerization) in the range of 450–4000 cm^{-1}.

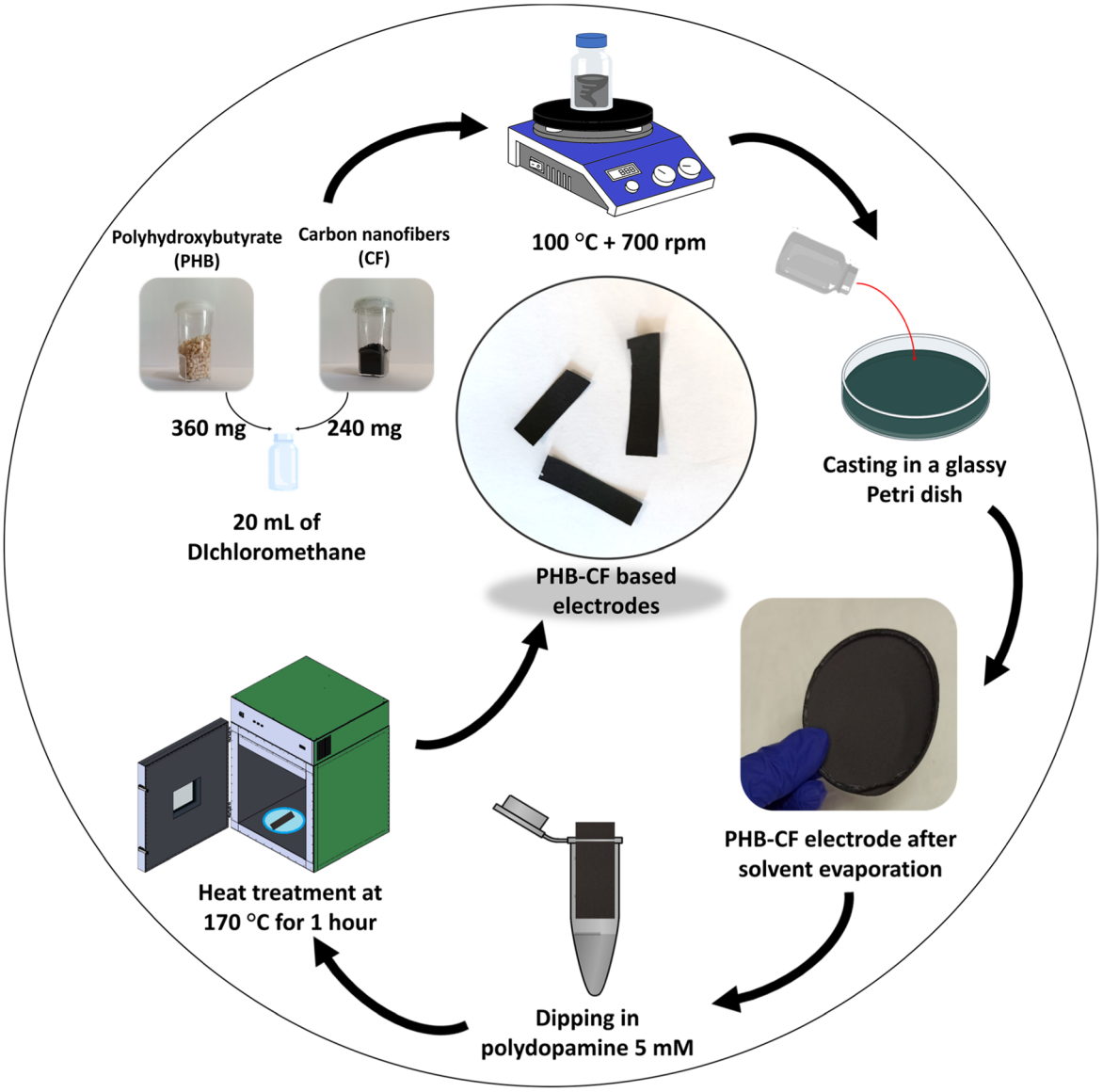

Scheme 1. Polyhydroxybutyrate-carbon nanofibers (PHB-CF) electrode preparation via casting process. PHB and CF are added in dichloromethane at 3:2 mass ratio. The suspension is heated and cast. The composite, free-standing, material obtained is dipped in a PDA solution and then heat-treated at 170 °C. Finally, the electrode material is cut into the desired shapes and dimensions.

Results and Discussion

Morphological characterization.—WCA measurement can be used as a good qualitative functional characterization of the wettability of the electrode surface. As reported in Fig. 1, the bare PHB-CF electrode surface can be considered as highly hydrophobic with an angle exceeding 120°. In all the measurements performed, a significant decrease of WCA was observed in the presence of the PDA layer on the electrode surface, which is associated with an increase in the hydrophilicity of the electrode. This can be considered as a desired property both for the electrochemical response of the PBH-CF electrodes in aqueous electrolytes and for the interaction of *R. capsulatus* cells with the electrode surface.

For biophotoanodes assembly, photosynthetic bacterial cells of *R. capsulatus* and dopamine solution were combined and spotted onto the PDA-PHB-CF electrodes. Dopamine polymerization started in aerobic conditions and was then finalized by repeated 20 cyclic voltammetry at the scan rates of 20 mV s^{-1}. During the electrochemical polymerization, in each CV cycle, a decrease of current density for the oxidative peak at a potential around +0.23 V is obtained due to the consumption of dopamine monomers to form the polydopamine matrix (Fig. 2). The current density at 0.23 V decreased over time from 740 ± 80 μA cm^{-2} (first cycle) to 80 ± 20 μA cm^{-2} after 20 cyclic voltammetry confirming the PDA formation. The experiments were performed also with control electrodes containing only PDA and heat-treated *R. capsulatus*, as shown in Fig. S1, providing a similar behavior.

ATR-FTIR spectroscopy reveals the presence of polydopamine on the electrode surface following PDA deposition and subsequent electrochemical polymerization via CV (Fig. 3). Some vibrational patterns exhibited similarities to both experimental and theoretical results for eumelanin.[64–66] The band between 650–675 cm^{-1} is attributed to the sp^2 amorphous phase activated by cooperative disorder within the sample, a characteristic shared with partially disordered carbon materials like polydopamine.[65] Moreover, these studies revealed overlaps between the bands associated with eumelanin-like structures and those of carbon materials, complicating their differentiation.[65] However, according to electrochemical analysis, Fig. 3B showed an increased intensity of this band across different electrodes, suggesting the presence of PDA on the electrode surface. Additionally, moderate intensity bands in the range of 2200–2400 cm^{-1} were exclusively

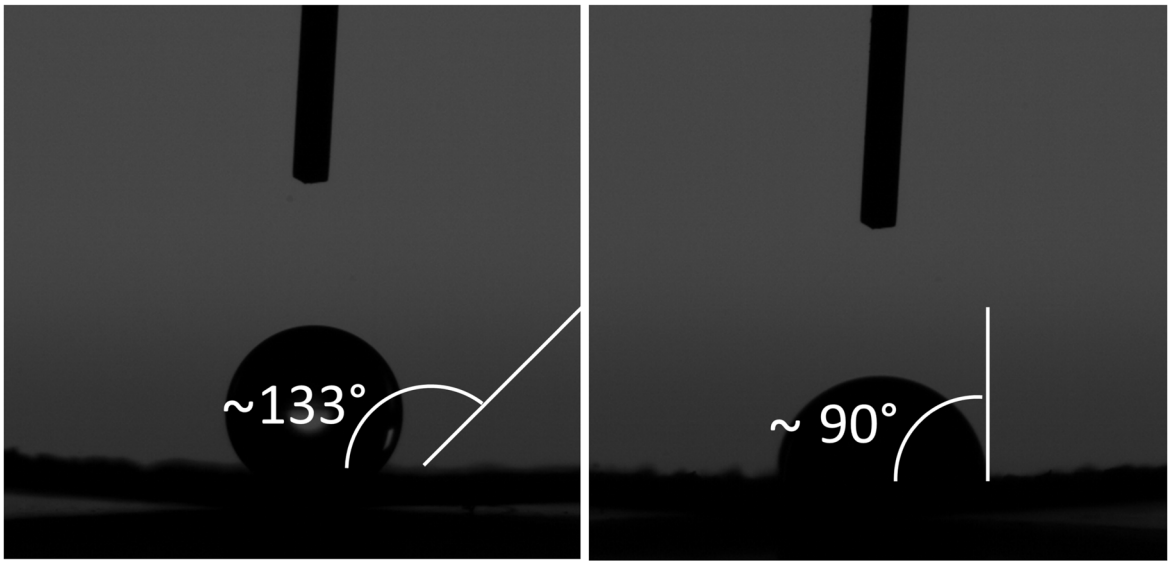

Figure 1. Water Contact Angle (WCA) images of the bare PHB-CF electrode (left) and the PHB-CF electrode modified with the PDA layer (right).

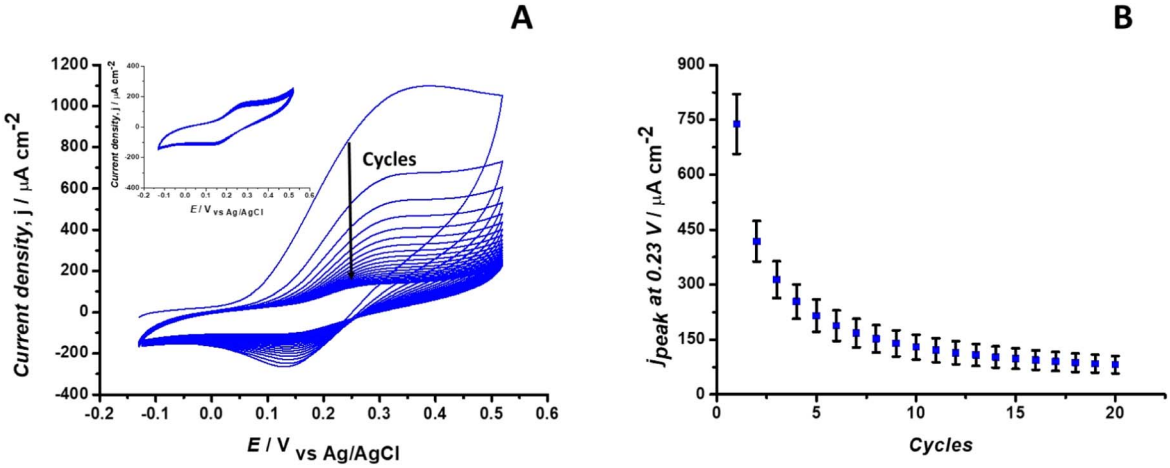

Figure 2. Electropolymerization of the PDA-*R. capsulatus* matrix for 20 cycles at the scan rate of 20 mV s^{-1}, reference electrode: AglAgCl (3 M NaCl). Current density measured at +0.23 V as function of the CV cycles (B). The inset shows the last five cyclic voltammetries for the bioelectrode with *R. capsulatus*.

observed in PHB-CF electrodes in contact with PDA (Fig. 3C). Further, in the following region functional groups typically associated with C-H stretching vibrations were observed, which can be aliphatic C-H groups, such as aromatic C-H stretching vibrations typical of dopamine polymers.[67,68]

The SEM micrograph of the PHB-CF composite electrodes highlighted the enhanced surface area of the highly porous material with interconnected carbon fibers (Fig. 4A). Surface modification with PDA was confirmed by the presence of the polymer homogeneously covering the carbon fibers (Fig. 4B). PHB-CF-PDA composite electrode with *R. capsulatus* cells (Fig. 4C) revealed that the bacterial cells on the electrode surface are organized in a highly dense biofilm, where single cell morphology was not distinguishable. At higher magnification (Fig. 4D), the dense bacterial layer onto the carbon fibers and single bacterial cells embedded into PDA were recognizable in the proximity of biofilm discontinuities, suggesting the biocompatibility of the developed substrate material with *R. capsulatus* cells.

Electrochemical characterization.—The photocatalytic activity of the PHB-CF-*R. capsulatus* hybrid bioelectrode was evaluated by cyclic voltammetry (CV) at 5 mV s^{-1} (Fig. 5) with malic acid serving as primary electron donor. The CV of the bioelectrode (black line) showed the characteristic redox peak of the polydopamine polymer at a potential of +0.23 V in agreement with values previously reported in the literature.[51] The hybrid bioelectrode showed a higher current density compared to the electrode prepared with heat-treated bacteria (red line) and bare electrode containing only polydopamine (grey line).[69,70] The comparison of the different electrodes is performed by evaluating the current density at +0.32 V as such conditions allow to reach quasi-steady-state currents. The bioanode exhibited a current density of 48 ± 10 μA cm^{-2} and 37 ± 3 μA cm^{-2} at +0.32 V under light and dark conditions, respectively. In contrast, the control PDA electrode showed low current density, achieving 15 ± 5 μA cm^{-2} and 12 ± 3 μA cm^{-2} at +0.32 V in the presence and absence of light, respectively. Similarly, the control electrode with heat-treated bacteria displayed a low photo response, probably due to light-response of polydopamine, with current density values of 10 ± 3 μA cm^{-2} and 7 ± 2 μA cm^{-2} under light and dark conditions, respectively. The results achieved by the biohybrid system can be attributed to the role of metabolically active *R. capsulatus* in the polydopamine layer, providing an increase in the catalytic activity of the matrix. Remarkably, our results confirmed that the PHB-CF electrode containing *R. capsulatus* electropolymerized with PDA generated higher current density in the presence of light.

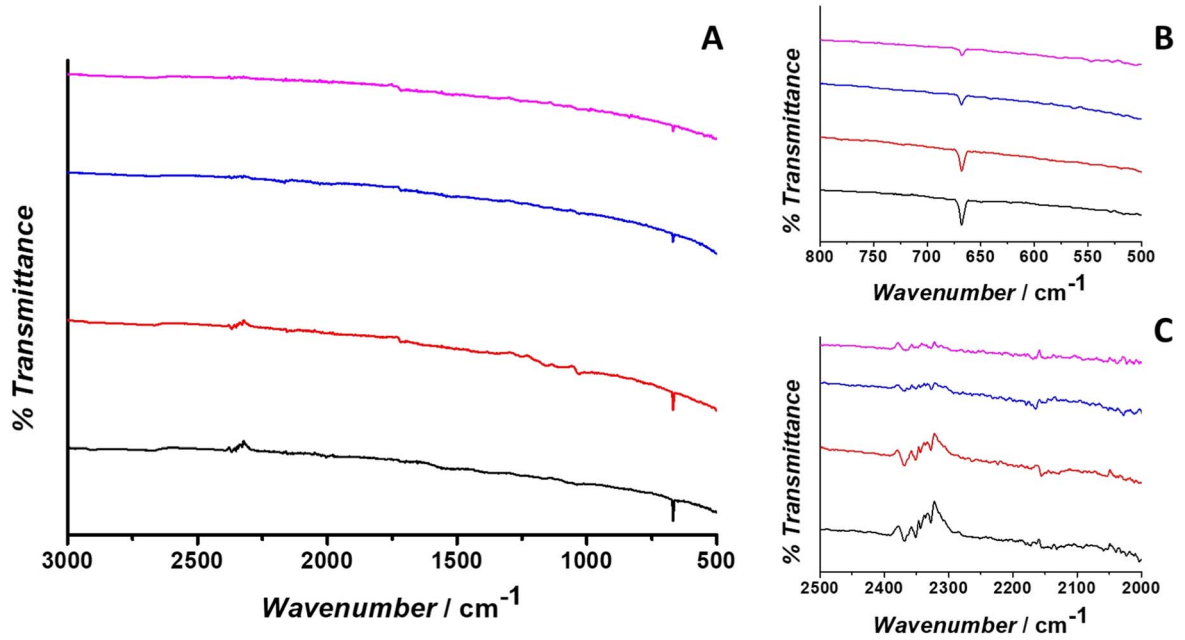

Figure 3. (A) ATR-FTIR spectra of bare PHB-CF electrode (pink line), PHB-CF heat treated electrode (blue line), PHB-CF after PDA deposition (red line), and PHB-CF after PDA electrochemical polymerization (black line). Magnification of the 500–800 cm^{-1} and the 2000–2500 cm^{-1} ranges (B and C, respectively).

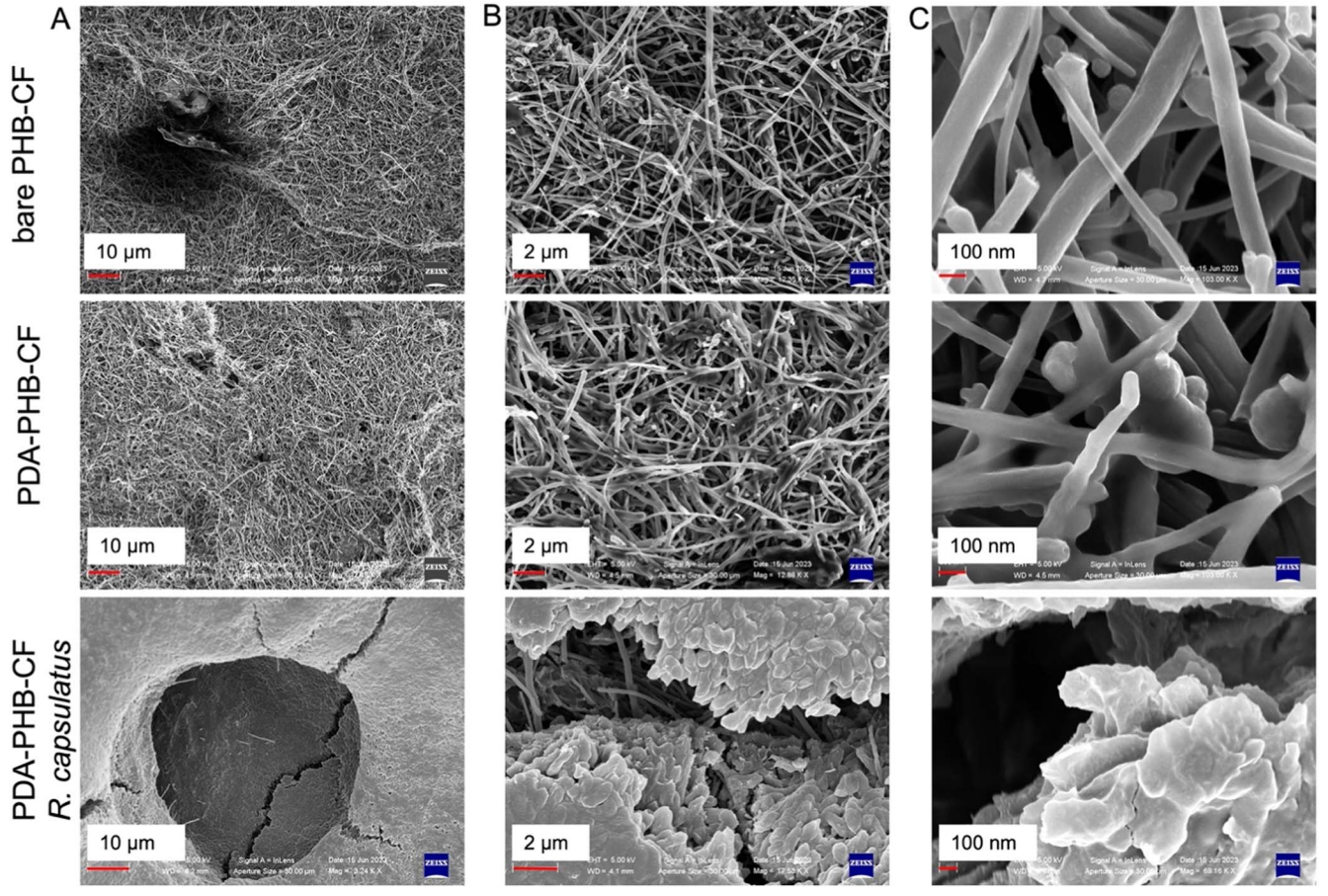

Figure 4. SEM images of the bare PHB-CF electrode, the PHB-CF electrode modified with the PDA layer, and the biohybrid PHB-CF electrode with *R. capsulatus* cells in the PDA matrix at 10 μm (A), 2 μm (B) and, 100 nm (C) magnification.

Following, chronoamperometry was utilized to evaluate the photocurrent after prolonged polarization of the electrodes at +0.32 V vs Ag|AgCl (3 M NaCl). As previously detailed, this potential was chosen based on the quasi-steady current obtained at this value. In Fig. 6, the system PHB-CF-*R. capsulatus* showed the highest current density, with an average value of 12 ± 3 μA cm^{-2} at

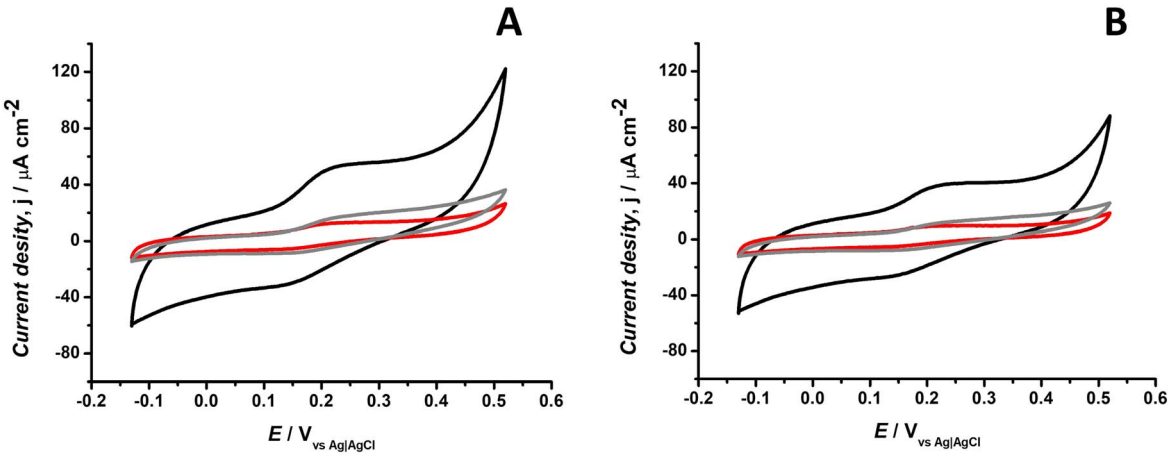

Figure 5. Cyclic voltammetry for the biophotoanode under light (A) and dark condition (B) for PDA-*R. capsulatus* (black line); PDA-*R. capsulatus* heat-treated (red line); only PDA (grey line). Scan rate, 5 mV s^{-1}; CE, Pt; RE, Ag | AgCl 3 M [NaCl.].

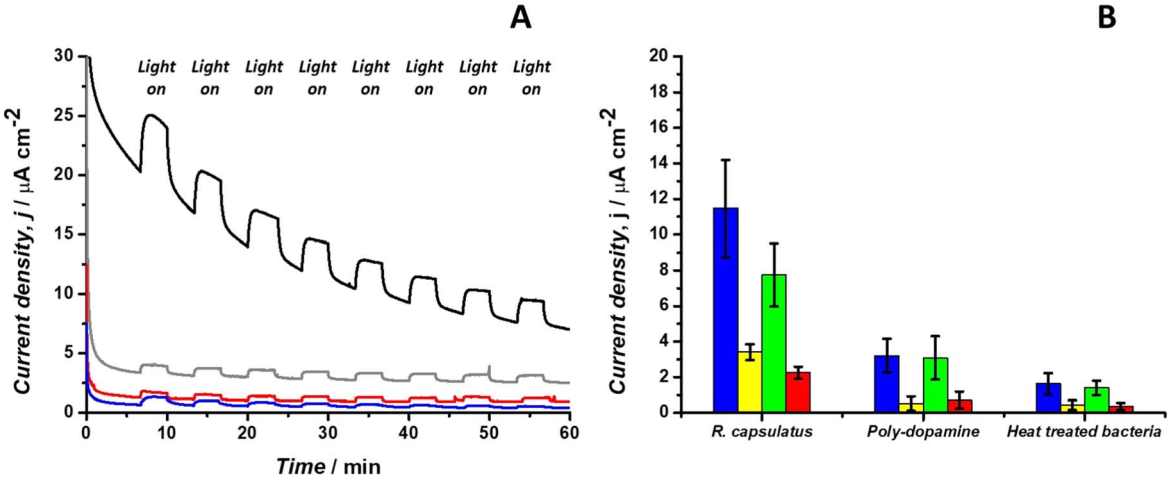

Figure 6. (A) Amperometric i-t traces at +0.32 V under light and dark conditions for the biophotoanode with PDA-*R. capsulatus* (black line), PDA-*R. capsulatus* heat-treated (red line), only PDA (grey line), and PDA-*R. capsulatus* on glassy carbon (blue line). (B) Comparison between overall current densities under light conditions (blue and green) and biophotocurrents (yellow and red) for: the fourth illumination cycle (blue and yellow bars) and the eighth cycle (green and red bars) for the biophotoanode with *R. capsulatus*, only dopamine, and heat-treated bacteria.

the fourth illumination cycle, corresponding to a bio-photocurrent of 3.4 ± 0.4 μA cm^{-2}. After prolonged operation, at the eighth illumination cycle, the system performance decreased, with a current density of 8 ± 2 μA cm^{-2} and a bio-photocurrent of 2.2 ± 0.3 μA cm^{-2}. The control test with only PDA and the metabolically inactivated bacteria confirmed the role of purple bacteria in the photocurrent generation. PDA, being a photoactive polymer, exhibited a current density value of 3 ± 1 μA cm^{-2}, with a photocurrent of 0.5 ± 0.4 μA cm^{-2}. In contrast, the heat-treated bacteria showed the lowest current response of 2 ± 1 μA cm^{-2}. This value was 2-fold lower compared with the electrode containing only PDA, possibly because the presence of inactive cells can disrupt the conductive matrix of PDA.

Figure 6 further highlights the performance of the hybrid biophotoanode over the prolonged operation, comparing the current density registered with the bio-photocurrents obtained. From the fourth to the eighth cycles, a reduction of 32 ± 1% is observed in current density terms. Similarly, a 34 ± 2% decrease in bio-photocurrent was obtained. The loss in (photo)current generation could be attributed to various factors, including a decrease in bacterial cell activity for the in situ generation of reactive oxygen species (ROS),[71–73] and electrode instability (i.e., possible slow detachment of bacterial cells from the electrode surface).

Based on the presented results, the joint action of the PDA, *R. capsulatus*, and the newly designed electrode PHB-CF allowed the high photocurrent generated by the assembled photobioelectrochemical system. The biobased material allowed improved adhesion of the PDA-bacteria matrix, with better performance over prolonged operation compared to glassy carbon electrodes (Fig. S6B). Notably, the biocompatible electrode had yielded an 18-fold increase in photocurrent generation,[51] when chronoamperometry experiments on glassy carbon resulted in a current density and biophotocurrent of 0.44 ± 0.08 μA cm^{-2} and 0.18 ± 0.08 μA cm^{-2} respectively. This breakthrough opens a wide array of electrochemical applications for this photoanode, ranging from biosensing to power generation.

Cost evaluation.—To ensure that the developed electrode is sustainable as well as cost-effective, an estimation of the cost to prepare the electrode has been performed and is reported in Table I. Comparing the price for every reactant in the electrode blend, the biopolymer polyhydroxybutyrate results to be the most cost-effective. Indeed, the average price for polyhydroxyalkanoates (PHAs) is 7.46 euros per Kg.[74] For the other components, carbon nanofibers have the highest influence on the final cost. The final price for a 1 cm^2 electrode is approximately 0.05 euros. Though this evaluation is based on cost and process considerations at a lab scale, it shows as

Table I. Cost analysis for the preparation of a batch of lab scale electrodes and 1 cm^2 electrode. Price referred to Carlo Erba reagents S.r.L and Merck KGaA's commercial catalogs. Polyhydroxybutyrate (PHB) stands out as the primary constituent in the blend, consistently maintaining its status as the most cost-effective component.

Products	Price/quantity	Quantity used	Cost (€)
Polyhydroxybutyrate[74]	7.46 € Kg^{-1}	360 mg	0.003 €
Carbon Nanofibers	7680 € Kg^{-1}	240 mg	1.84 €
Dichloromethane	29.61 € L^{-1}	20 mL	0.59 €
47 cm^2 PHB-CF electrode (lab scale)			2.43 €
1 cm^2 PHB-CF electrode			0.05 €

the development of small bioelectrochemical devices with PHB-based electrodes for different applications, such as biosensing, would be particularly accessible, enabling their use as disposable and on-demand systems.

Conclusions

A novel blend of polyhydroxybutyrate and carbon nanofibers was introduced as a promising, eco-friendly, and biocompatible material for free-standing electrodes in bioelectrochemical systems. The present biophotoanode demonstrates a current density of 12 ± 3 $\mu A\ cm^{-2}$ and a substantial bio-photocurrent production of 3.4 ± 0.4 $\mu A\ cm^{-2}$. In comparison to commercial glassy carbon electrode, which yielded a current density of 0.44 ± 0.08 $\mu A\ cm^{-2}$ and a biophotocurrent of 0.18 ± 0.08 $\mu A\ cm^{-2}$, the biophotoanode exhibits a remarkable 18-fold enhancement in performance. This underscores the promising potential of the polyhydroxybutyrate-carbon nanofiber blend in advancing the efficiency and sustainability of microbial electrochemical systems, targeting cost-effective devices that could be deployed in the environment.

Acknowledgments

J. H. Franco and M. Grattieri would like to acknowledge the funding from Fondazione CON IL SUD, Grant "Brains to South 2018," project number 2018-PDR-00914. l.D.M. Torquato would like to thank Fundação de Amparo à Pesquisa do Estado de São Paulo (FAPESP) for funding under grant number 2021/09471–2. R. Labarile and M. Trotta acknowledges funding from Fonds National Suisse de la Recherche Scientifique, project Phosbury—Photosynthetic bacteria in Self-assembled Biocompatible coatings for the transduction of energy (Project Nr CRSII5_205925/1). M. Trotta acknowledges the project PrinPNRR2022—P20225NFS4 (PhOLcs—Photosynthesis for Organic Light-Powered Electronics). D. Lacalamita would like to thank ENI SPA for the PhD fellowship "Da acque reflue a H_2 per bioelettrolisi microbica."

ORCID

Lilian Danielle de Moura Torquato https://orcid.org/0000-0003-2907-2617
Dario Lacalamita https://orcid.org/0000-0002-4819-1104
Rosa Maria Matteucci https://orcid.org/0009-0001-2675-1860
Jefferson Honorio Franco https://orcid.org/0000-0002-1170-5108
Rossella Labarile https://orcid.org/0000-0003-0717-3679
Alberto Perrotta https://orcid.org/0000-0002-7007-6153
Massimo Trotta https://orcid.org/0000-0002-8220-4597
Gianluca Maria Farinola https://orcid.org/0000-0002-1601-2810
Maria Valnice Boldrin Zanoni https://orcid.org/0000-0002-2296-1393
Matteo Grattieri https://orcid.org/0000-0002-1795-3655
Paolo Stufano https://orcid.org/0000-0002-4571-0482

References

1. G. Bedendi, L. D. De Moura Torquato, S. Webb, C. Cadoux, A. Kulkarni, S. Sahin, P. Maroni, R. D. Milton, and M. Grattieri, *ACS Meas. Sci. Au.*, **2**, 517 (2022).
2. S. A. Patil, C. Hägerhäll, and L. Gorton, *Bioanalytical Reviews*, **4**, 159 (2012).
3. S. Mohle, M. Zirbes, E. Rodrigo, T. Gieshoff, A. Wiebe, and S. R. Waldvogel, *Angew. Chem. Int. Ed. Engl.*, **57**, 6018 (2018).
4. G. Pankratova and L. Gorton, *Current Opinion in Electrochemistry*, **5**, 193 (2017).
5. S. Cestellos-Blanco, H. Zhang, J. M. Kim, Y.-X. Shen, and P. Yang, *Nat. Catal.*, **3**, 245 (2020).
6. M. Rasmussen and S. D. Minteer, *J. Electrochem. Soc.*, **161**, H647 (2014).
7. S. Bajracharya, M. Sharma, G. Mohanakrishna, X. Dominguez Benneton, D. P. B. T.-B. Strik, P. M. Sarma, and D. Pant, *Renewable Energy*, **98**, 153 (2016).
8. L. Xiao and Z. He, *Renew. Sustain. Energy Rev.*, **37**, 550 (2014).
9. K. G. Satyanarayana, A. B. Mariano, and J. V.-C. Vargas, *Int. J. Energy Res.*, **35**, 291 (2011).
10. N. Kornienko, J. Z. Zhang, K. K. Sakimoto, P. Yang, and E. Reisner, *Nat. Nanotechnol.*, **13**, 890 (2018).
11. K. Hasan, V. Grippo, E. Sperling, M. A. Packer, D. Leech, and L. Gorton, *ChemElectroChem*, **4**, 412 (2017).
12. D. Pankratov, G. Pankratova, T. P. Dyachkova, P. Falkman, H.-E. Åkerlund, M. D. Toscano, Q. Chi, and L. Gorton, *ACS Energy Lett.*, **2**, 2635 (2017).
13. K. L. Saar, P. Bombelli, D. J. Lea-Smith, T. Call, E.-M. Aro, T. Müller, C. J. Howe, and T. P.-J. Knowles, *Nat. Energy*, **3**, 75 (2018).
14. R. Labarile, D. Vona, M. Varsalona, M. Grattieri, M. Reggente, R. Comparelli, G. M. Farinola, F. Fischer, A. A. Boghossian, and M. Trotta, *Nano Res.*, **17**, 875 (2024).
15. M.-J. Choi, E. Yang, H.-W. Yu, I. S. Kim, S.-E. Oh, and K.-J. Chae, *Int. J. Hydrogen Energy*, **44**, 2258 (2019).
16. B. De Gusseme, T. Hennebel, L. Vanhaecke, M. Soetaert, J. Desloover, K. Wille, K. Verbeken, W. Verstraete, and N. Boon, *Environ. Sci. Technol.*, **45**, 5737 (2011).
17. B. Qiu, Y. Hu, C. Liang, L. Wang, Y. Shu, Y. Chen, and J. Cheng, *Bioresour. Technol.*, **300**, 122703 (2020).
18. B. Qiu, Y. Hu, C. Tang, Y. Chen, and J. Cheng, *Sci. Total Environ.*, **792**, 148446 (2021).
19. P. A. Selembo, M. D. Merrill, and B. E. Logan, *Int. J. Hydrogen Energy*, **35**, 428 (2010).
20. M. M. Mardanpour and S. Yaghmaei, *Biosens. Bioelectron.*, **79**, 327 (2016).
21. M. Gebresemati, G. Das, B. J. Park, and H. H. Yoon, *Int. J. Hydrogen Energy*, **42**, 29874 (2017).
22. H. Feng, Y. Liang, K. Guo, W. Chen, D. Shen, L. Huang, Y. Zhou, M. Wang, and Y. Long, *Environmental Science & Technology Letters*, **3**, 420 (2016).
23. U. Michaelidou, A. ter Heijne, G. J. Euverink, H. V. Hamelers, A. J. Stams, and J. S. Geelhoed, *Appl. Environ. Microbiol.*, **77**, 1069 (2011).
24. X. Ying, D. Shen, M. Wang, H. Feng, Y. Gu, and W. Chen, *Chem. Eng. J.*, **333**, 260 (2018).
25. M. Muhyuddin, N. Zocche, R. Lorenzi, C. Ferrara, F. Poli, F. Soavi, and C. Santoro, *Mater. Renew. Sustain. Energy*, **11**, 131 (2022).
26. O. Simoska, E. M. Gaffney, S. D. Minteer, A. Franzetti, P. Cristiani, M. Grattieri, and C. Santoro, *Current Opinion in Electrochemistry*, **30**, 100762 (2021).
27. Z. Hassanvand, F. Jalali, M. Nazari, F. Parnianchi, and C. Santoro, *Chem. Electro. Chem*, **8**, 15 (2021).
28. C. Santoro, M. Kodali, S. Kabir, F. Soavi, A. Serov, and P. Atanassov, *J. Power Sources*, **356**, 371 (2017).
29. F. Soavi, L. G. Bettini, P. Piseri, P. Milani, C. Santoro, P. Atanassov, and C. Arbizzani, *J. Power Sources*, **326**, 717 (2016).
30. H. Lyu, Z. Yu, B. Gao, F. He, J. Huang, J. Tang, and B. Shen, *Environ. Sci. Pollut. Res. Int.*, **26**, 14693 (2019).
31. P. Manasa, S. Sambasivam, and F. Ran, *Journal of Energy Storage*, **54**, 105290 (2022).
32. J. L. Goldfarb, G. Dou, M. Salari, and M. W. Grinstaff, *ACS Sustainable Chemistry & Engineering*, **5**, 3046 (2017).
33. S. ul Haque, A. Nasar, N. Duteanu, S. Pandey, and Inamuddin, *Fuel*, **331**, 125634 (2023).
34. M. Mehmandoust, G. Li, and N. Erk, *Ind. Eng. Chem. Res.*, **62**, 4628 (2022).
35. N. S. Weliwatte, M. Grattieri, O. Simoska, Z. Rhodes, and S. D. Minteer, *Langmuir*, **37**, 7821 (2021).
36. J. N. Roy, H. R. Luckarift, S. R. Sizemore, K. E. Farrington, C. Lau, G. R. Johnson, and P. Atanassov, *Enzyme Microb. Technol.*, **53**, 123 (2013).
37. H. R. Luckarift, S. R. Sizemore, K. E. Farrington, J. Roy, C. Lau, P. B. Atanassov, and G. R. Johnson, *ACS Appl. Mater. Interfaces*, **4**, 2082 (2012).
38. Y. Nishio, D.-T. Nguyen, and K. Taguchi, *Energy Reports*, **9**, 66 (2023).
39. C. Kourmentza, J. Placido, N. Venetsaneas, A. Burniol-Figols, C. Varrone, H. N. Gavala, and M. A.-M. Reis, *Bioengineering (Basel)*, **4**, 55 (2017).

40. V. Montiel-Corona and G. Buitron, *Bioresour. Technol.*, **373**, 128704 (2023).
41. E. Orsi, P. L. Folch, V. T. Monje-Lopez, B. M. Fernhout, A. Turcato, S. W.-M. Kengen, G. Eggink, and R. A. Weusthuis, *J. Ind. Microbiol. Biotechnol.*, **46**, 1179 (2019).
42. G. Policastro, V. Luongo, and M. Fabbricino, *J. Environ. Manage.*, **271**, 111006 (2020).
43. S. Sali and H. R. Mackey, *Reviews in Environmental Science and Bio/Technology*, **20**, 959 (2021).
44. M. Koller, L. Marsalek, M. M. de Sousa Dias, and G. Braunegg, *N Biotechnol*, **37**, 24 (2017).
45. V. Sharma, R. Sehgal, and R. Gupta, *Polymer*, **212**, 123161 (2021).
46. M. Zinn, B. Witholt, and T. Egli, *Adv. Drug Delivery Rev.*, **53**, 5 (2001).
47. P. Phukon, K. Radhapyari, B. K. Konwar, and R. Khan, *Mater. Sci. Eng. C: Mater. Biol. Appl.*, **37**, 314 (2014).
48. A. A.-O. Sirajudeen, M. S.-M. Annuar, and R. Subramaniam, *Biotechnol. Appl. Biochem.*, **68**, 307 (2021).
49. H. Niu, J. Zhang, Z. Xie, X. Wang, and T. Lin, *Carbon*, **49**, 2380 (2011).
50. D. Yadav, F. Amini, and A. Ehrmann, *Eur. Polym. J.*, **138**, 109963 (2020).
51. G. Buscemi, D. Vona, P. Stufano, R. Labarile, P. Cosma, A. Agostiano, M. Trotta, G. M. Farinola, and M. Grattieri, *ACS Appl. Mater. Interfaces*, **14**, 26631 (2022).
52. C. Manchon, F. Muniesa-Merino, D. Serna, Y. Asensio, C. Wardman, and A. Esteve-Nuñez, *Chem. Eng. J.*, **453**, 139828 (2023).
53. M. Grattieri, R. Labarile, G. Buscemi, and M. Trotta, *Photochem. Photobiol. Sci.*, **21**, 101 (2022).
54. I. A. Vasiliadou, A. Berná, C. Manchon, J. A. Melero, F. Martinez, A. Esteve-Nuñez, and D. Puyol, *Frontiers in Energy Research*, **6**, 107 (2018).
55. S. Li, M. Sakuntala, Y. E. Song, J. O. Heo, M. Kim, S. Y. Lee, M. S. Kim, Y. K. Oh, and J. R. Kim, *Bioresour. Technol.*, **320**, 124333 (2021).
56. M. Grattieri and S. D. Minteer, *ACS Sens.*, **3**, 44 (2018).
57. K. Hasan, S. A. Patil, K. Gorecki, D. Leech, C. Hagerhall, and L. Gorton, *Bioelectrochemistry*, **93**, 30 (2013).
58. K. Hasan, K. V.-R. Reddy, V. Eßmann, K. Górecki, P. Ó. Conghaile, W. Schuhmann, D. Leech, C. Hägerhäll, and L. Gorton, *Electroanalysis*, **27**, 118 (2015).
59. M. Grattieri, S. Patterson, J. Copeland, K. Klunder, and S. D. Minteer, *Chem. Sus. Chem*, **13**, 230 (2020).
60. K. Beaver, E. M. Gaffney, and S. D. Minteer, *Electrochim. Acta*, **416**, 140291 (2022).
61. K. Beaver, A. Dantanarayana, A. B. Zani, D. L. Lehto, and S. D. Minteer, *J. Electrochem. Soc.*, **170**, 045503 (2023).
62. M. Grattieri, K. Beaver, E. M. Gaffney, and S. D. Minteer, *Faraday Discuss.*, **215**, 15 (2019).
63. M. Grattieri, Z. Rhodes, D. P. Hickey, K. Beaver, and S. D. Minteer, *ACS Catal.*, **9**, 867 (2019).
64. J. Liebscher, R. Mrowczynski, H. A. Scheidt, C. Filip, N. D. Hadade, R. Turcu, A. Bende, and S. Beck, *Langmuir*, **29**, 10539 (2013).
65. E. Coy, I. Iatsunskyi, J. C. Colmenares, Y. Kim, and R. Mrowczynski, *ACS Appl. Mater. Interfaces*, **13**, 23113 (2021).
66. R. A. Zangmeister, T. A. Morris, and M. J. Tarlov, *Langmuir*, **29**, 8619 (2013).
67. F. Yu, S. Chen, Y. Chen, H. Li, L. Yang, Y. Chen, and Y. Yin, *J. Mol. Struct.*, **982**, 152 (2010).
68. B. Stöckle, D. Y.-W. Ng, C. Meier, T. Paust, F. Bischoff, T. Diemant, R. J. Behm, K. E. Gottschalk, U. Ziener, and T. Weil, *Macromolecular Symposia*, **346**, 73 (2014).
69. S. Shleev, E. González-Arribas, and M. Falk, *Current Opinion in Electrochemistry*, **5**, 226 (2017).
70. X. Long, H. Wang, C. Wang, and X. Li, *Environ. Technol.*, **41**, 3420 (2020).
71. A. Ruff, F. Conzuelo, and W. Schuhmann, *Nat. Catal.*, **3**, 214 (2019).
72. F. Zhao, A. Ruff, M. Rogner, W. Schuhmann, and F. Conzuelo, *J. Am. Chem. Soc.*, **141**, 5102 (2019).
73. F. Zhao, S. Hardt, V. Hartmann, H. Zhang, M. M. Nowaczyk, M. Rogner, N. Plumere, W. Schuhmann, and F. Conzuelo, *Nat. Commun.*, **9**, 1973 (2018).
74. B. Alvarez Chavez, V. Raghavan, and B. Tartakovsky, *RSC Adv.*, **12**, 16105 (2022).